Prediction of Damage Initiation and Simulation of Damage Propagation in 3D Woven Composites During Processing

DMYTRO KUKSENKO, BORYS DRACH, and IGOR TSUKROV

ABSTRACT

Some configurations of 3D woven composites are known to be susceptible to processing induced damage in the form of microcracks that develop in the polymer matrix during curing. The microcracking is believed to originate from high residual stresses that develop due to a significant mismatch in the coefficients of thermal expansion between the constituent materials. In this paper, we investigate the applicability of several commonly used stress-based failure criteria for glassy polymers – the von Mises, the Bauwens (Drucker-Prager), the parabolic stress, and the dilatational strain energy density. We study the microcracking phenomenon on the example of the one-to-one orthogonal configuration of the epoxy matrix/carbon fiber 3D woven composites. This configuration is characterized by the high level of the through-thickness reinforcement which appears to exacerbate the matrix damage.

The investigation is based on a high-fidelity mesoscale finite element model of an orthogonally reinforced 3D woven composite. We simulate the material's response to the uniform temperature drop from the curing to room temperature and compare the results of the simulation with the X-ray computed microtomography. We conclude that the curing induced matrix failure is well predicted by the parabolic stress criterion with a proper choice of the material constants. Initiation and propagation of this failure are simulated via sequential deactivation of the elements exceeding the allowable equivalent stress.

INTRODUCTION

The advantages of 3D woven composites over the traditional 2D woven composite laminates include continuous reinforcement in all three dimensions, high strength and fatigue resistance under multiaxial loading. However, some 3D woven composite

Dmytro Kuksenko, Mechanical & Aerospace Eng., New Mexico State Univ., Las Cruces, NM
Borys Drach, Mechanical & Aerospace Eng., New Mexico State Univ., Las Cruces, NM
Igor Tsukrov, Mechanical Eng., Univ. of New Hampshire, Durham, NH

material systems are known to be susceptible to curing induced matrix microcracking during manufacturing. Figure 1 shows microcracks that developed in a 3D woven carbon/epoxy composite with the reinforcement configuration studied in this paper. Based on the observations, we assume that the major factor in process-induced microcracking of woven composites is the residual stress due to mismatch of the thermal expansion coefficients (CTEs) between carbon fibers and epoxy matrix that develops when completely cured matrix cools from the curing to room temperature.

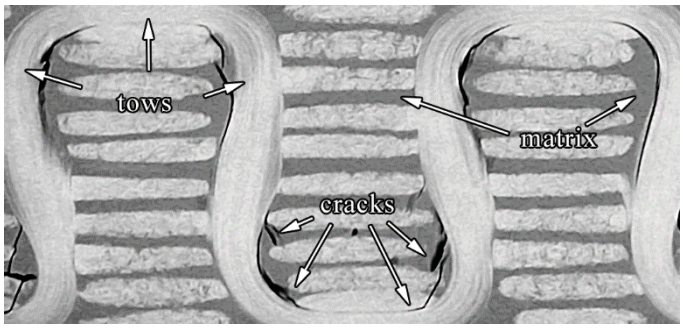

Figure 1. X-ray computed microtomography image of a 3D woven composite with one-to-one orthogonal reinforcement showing microcracks in the matrix due to curing

This paper presents a finite element analysis study to quantify the residual stresses due to cooling after curing in the one-to-one orthogonally reinforced 3D woven composite. The finite element model for the analysis was developed following the procedure detailed in [1]. We compare the numerically predicted failure areas based on several commonly used failure criteria with X-ray computed microtomography data to investigate the applicability of these criteria to the composite system in question. We assume that the residual stresses responsible for the microcracking arise solely due to the mismatch in CTEs between the matrix and the tows, and ignore the chemical shrinkage contribution as suggested in [2]. In addition, we simulate progressive damage via sequential deactivation of elements exceeding allowable stresses. The temperature dependent thermo-mechanical properties of the RTM6 epoxy resin reported in [2] are used. The reinforcement tows are assigned the effective properties of IM7 carbon fiber bundles embedded in the resin matrix, see homogenization approaches presented in [3], [4] and [5].

We begin our presentation with the discussion of the four commonly used stress-based failure criteria considered for damage initiation predictions. In the next section, we outline our approach to preparation of the mesoscale finite element model and assignment of the temperature-dependent material properties. We then present the results of the simulation of cooling after curing in the absence of damage propagation. In the same section, we compare the processing-induced stress concentrations with the damage observations obtained using the X-ray computed microtomography performed on the actual composite specimen of the same configuration. Later, we simulate the initiation and propagation of damage via the sequential deactivation of elements exceeding the allowable stresses. In the final section, we present the conclusions of this research.

FAILURE CRITERIA

The criteria considered in this paper for damage initiation predictions in 3D woven composites with epoxy matrix include the von Mises, dilatational energy, parabolic and Bauwens (Drucker-Prager). They are formulated as follows.

Von Mises criterion assumes that the material will not yield if the equivalent stress calculated as $\sigma_{VM} = \sqrt{0.5\,[(\sigma_1 - \sigma_2)^2 + (\sigma_1 - \sigma_3)^2 + (\sigma_2 - \sigma_3)^2]}$ is below the critical value:

$$\sigma_{VM} \leq \sigma_{VM}^{crit} \tag{1}$$

where $\sigma_1, \sigma_2, \sigma_3$ are the principal stresses. In our simulations, we use the critical value $\sigma_{VM}^{crit} = 67.8\ MPa$ chosen based on the measurements reported in [2].

Dilatational energy criterion is based on the energy required for crack initiation by void nucleation. Assuming linear material behavior, the stress energy density is calculated as

$$U_v = \frac{1-2\nu}{6E}(\sigma_1 + \sigma_2 + \sigma_3)^2 \tag{2}$$

where E is the Young's modulus and ν is the Poisson's ratio of the material. This criterion can be re-written as

$$\sigma_H \leq \sigma_H^{crit}, \tag{3}$$

where $\sigma_H = \frac{1}{3}(\sigma_1 + \sigma_2 + \sigma_3)$ is the hydrostatic stress, and σ_H^{crit} is the value of hydrostatic stress that corresponds to the critical energy density required for cavitation. The approaches to determine this value include the poker chip experiments [6]–[8], the constrained tube method [9], [10] and evaluation of σ_H^{crit} from uniaxial tensile tests [10]. We use the value $\sigma_H^{crit} = 58.7\ MPa$ based on the estimate $U_v^{crit} = 0.4\ MPa$ for RTM6 epoxy provided in [11].

Parabolic failure criterion was utilized in [12] based on the description provided in [13]. It combines the first and the second invariants of stress as

$$\sigma_{VM}^2 + A\,\sigma_H \leq B^{crit} \tag{4}$$

The material parameters A and B^{crit} are found from mechanical testing of the material. Asp et al. [11] provide failure stresses for RTM6 in tension and compression as $\sigma_{yt} = 82\ MPa$ and $\sigma_{yc} = 134\ MPa$. Based on these values we obtain $A = 156\ MPa$ and $B^{crit} = 10{,}990\ (MPa)^2$.

Bauwens (Drucker-Prager) criterion uses a linear combination of von Mises and hydrostatic stress to predict failure [13]:

$$\sigma_{VM} + C\,\sigma_H \leq D^{crit} \tag{5}$$

Based on tension and compression results provided in [11], the material parameters are chosen as $C = 0.722$ and $D^{crit} = 50.9\ MPa$.

GEOMETRY AND FINITE ELEMENT MODEL PREPARATION

We focus on the one-to-one orthogonally reinforced composite panel consisting of ten layers of warp and weft tows with a through-thickness binder tow as can be seen in Figure 1 and Figure 2. The panel thickness is 4.1mm, and the in-plane dimensions of the unit cell are 5.1x5.1mm. The geometry of the unit cell is generated based on the fabric mechanics simulations performed using DFMA software developed by Wang et al. [14]-[16]. In the simulations, the process starts with generating an initial pattern of the reinforcement architecture based on the weave pattern, the number of tows, their areas and spacing, see Figure 2a. The tows in the initial pattern (represented by single cylindrical fibers each) are then subdivided into sub-tows and subjected to tensile forces. The relaxation of these forces mimics the weaving process of the 3D woven reinforcement. For better accuracy, the number of sub-tows can be increased and relaxed multiple times until a realistic reinforcement geometry is achieved.

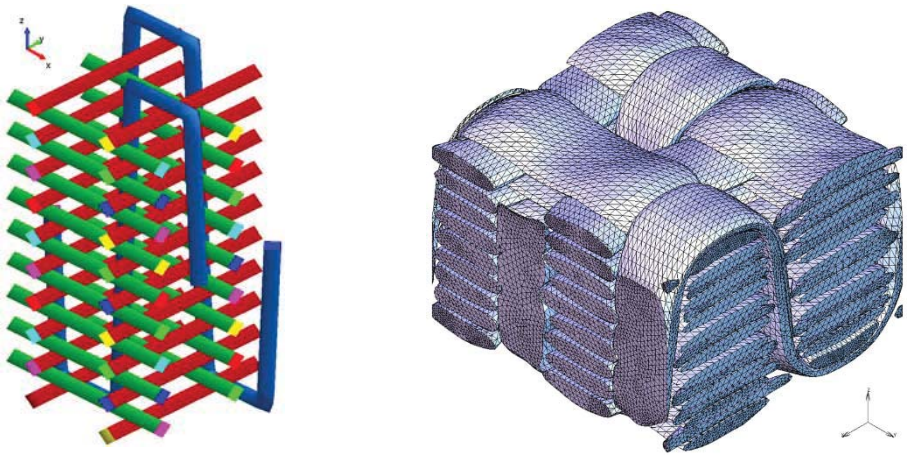

(a) (b)

Figure 2. (a) Weave pattern of the one-to-one orthogonal reinforcement architecture (DFMA); (b) finite element mesh of the composite unit cell (shown: reinforcement without the matrix)

The FE mesh of the composite's unit cell (UC) is developed using a custom MATLAB script based on the DFMA results and imported into the commercial FEA software MSC Marc Mentat, see [1], [17] for details. Periodic boundary conditions are prescribed on the external lateral surfaces of the UC to preserve the material continuity on the macroscale. There is no periodicity in the thickness direction because the entire panel thickness is represented by the UC. All model preparation steps are performed automatically within the MSC Mentat software using a custom Python script. At the completion of the script, the user is presented with a ready-to-run model.

The matrix phase (fully cured HEXCEL RTM6 epoxy resin) is simulated as a linear isotropic material with constant Poisson's ratio $\nu_m = 0.35$, and temperature dependent Young's modulus and thermal expansion coefficient [2]:

$$E_m = E_m^{0℃} - \beta_m T \tag{6}$$

$$\alpha_m = \alpha_m^{0℃} + \gamma_m T \tag{7}$$

where $E_m^{0℃} = 3{,}500\ MPa$, $\beta_m = 5.9 \frac{MPa}{℃}$, $\alpha_m^{0℃} = 5 \cdot 10^{-5} \frac{1}{K}$, $\gamma_m = 1.05 \cdot 10^{-7} \frac{1}{K \cdot ℃}$ are the material parameters, and T is the temperature in $°C$.

The tows consist of 12K IM7 carbon fibers impregnated with RTM6 epoxy. The volume fraction of fibers within the tows is set to 80%. Based on the fiber properties provided in [18] and the resin properties $E_m = 2.89\ GPa, \nu_m = 0.35, \alpha_m = 65 \cdot 10^{-6} \frac{1}{K}$ given in Table 2 of [2], the following properties of the tow are obtained: $E_{1t} = 221.38\ GPa, E_{2t} = 13.18\ GPa, G_{12t} = 7.17\ GPa, \nu_{12t} = 0.35, \nu_{23t} = 0.35, \alpha_{1t} = -2.29 \cdot 10^{-7} \frac{1}{K}, \alpha_{2t} = 2.23 \cdot 10^{-5} \frac{1}{K}$. Note that the properties of the matrix in the tows change during curing with temperature, see formulas 6 and 7. However, due to low volume fraction and Young's modulus of the matrix (compared to the carbon fibers) these changes will result in insignificant variations of the homogenized properties of the tows, so in the numerical simulations the properties of the tows are assumed to be temperature independent.

PREDICTIONS OF RESIDUAL STRESSES AFTER CURING

Numerical simulations of cooling after curing of the composite were performed to predict the development of the residual stresses. It was assumed that the material is fully cured and stress-free in the beginning of the simulation at the curing temperature $T_0 = 165\ °C$. The entire UC is then cooled uniformly from curing to room temperature by prescribing a temperature drop of $\Delta T = -140\ °C$ over 40 steps.

Figure 3 presents numerically predicted distributions of the equivalent stresses in the cross-section of the middle of the binder tow perpendicular to the weft direction. It can be seen that von Mises stress criterion (the corresponding distribution is given in panel (c)) predicts damage on the convex surfaces of the binder tow while the actual composite contains microcracks on the concave sides. It is also evident that Bauwens criterion (panel (d)) significantly overpredicts the extent of damage showing the entire resin volume to be above the critical value. Both parabolic (panel (e)) and dilatational energy (panel (f)) criteria appear to correctly predict the locations of the damaged regions within the unit cell. It appears that the actual damaged area is larger than what is predicted by the parabolic criterion but smaller than what is predicted by the dilatational energy criterion. Therefore, it is difficult to say definitively which of the two (parabolic stress or dilatational energy) is a better choice. Note that propagation of damage is not included in this section, which might have affected the predictions. On one hand, cracks when formed would alleviate the stress concentrations on the constituent materials' interfaces and limit the extent of further damage to the surrounding matrix. At the same time the crack fronts may produce very high stress concentrations which might result in rapid propagation of the cracks through the composite thickness. In the next section, we investigate progressive damage modeled via sequential element deactivation based on the parabolic failure criterion. Note that application of the dilatational energy criterion is presented elsewhere [19].

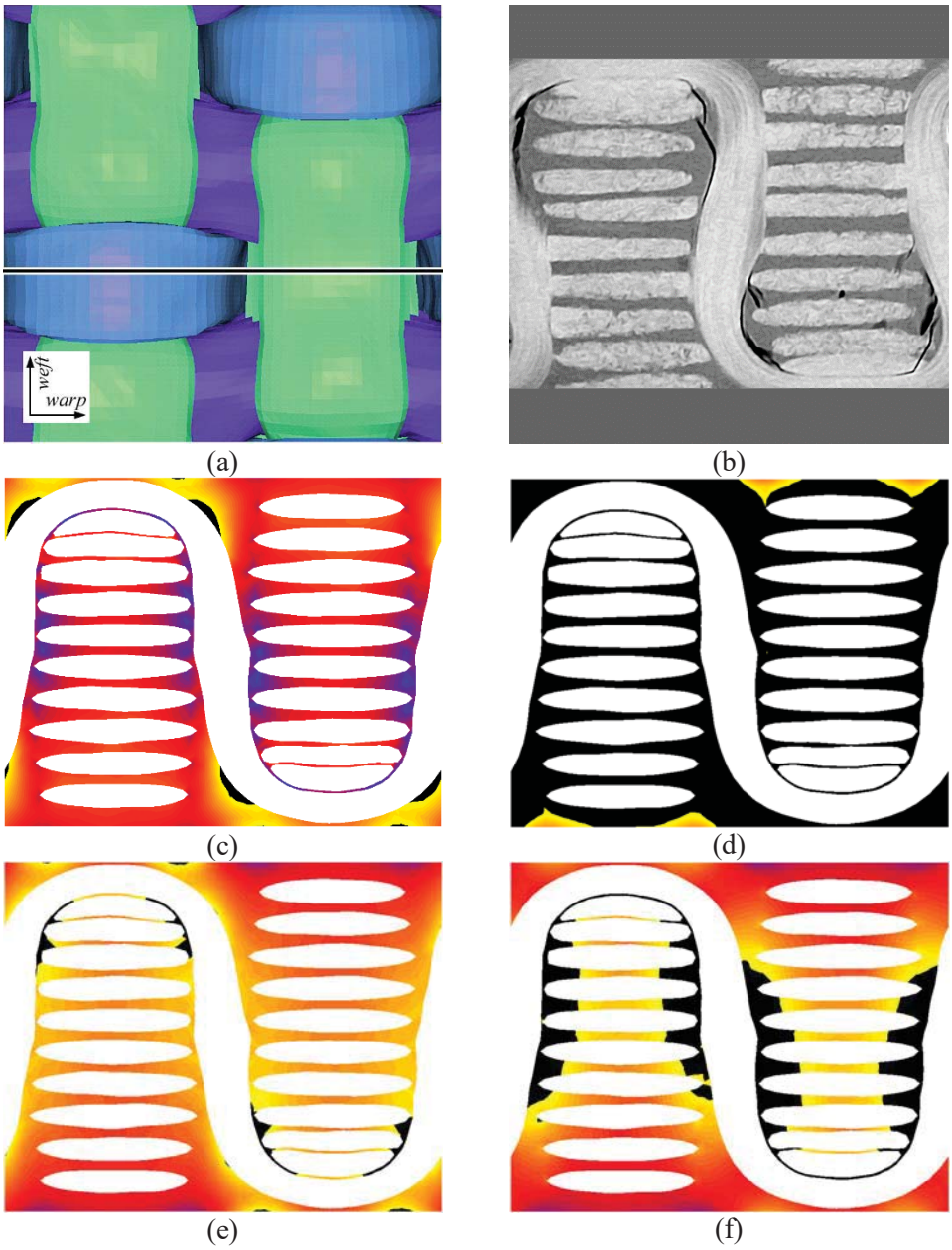

Figure 3. Distribution of the equivalent stresses in the matrix of the UC after cooling: (a) slice location within the UC; (b) microtomography image; (c) von Mises; (d) Bauwens; (e) parabolic criterion with coefficients based on [11]; (f) dilatational energy criterion. The colormap ranges from blue (zero) to yellow with regions above critical value shown in black

DAMAGE MODELING VIA ELEMENT DEACTIVATION

In this section, we model the propagation of damage in the composite during cooling after curing via deactivation of the elements exceeding the allowable parabolic stress. The damaged unit cell is shown in Figure 4. From the comparison of the stress concentration result (Figure 4c) with the simulation of damage propagation (Figure 4d) it appears that crack fronts indeed produce very high stress concentrations

as was hypothesized in the previous section. This in turn leads to a greater extent of the damage compared to the results without element deactivation.

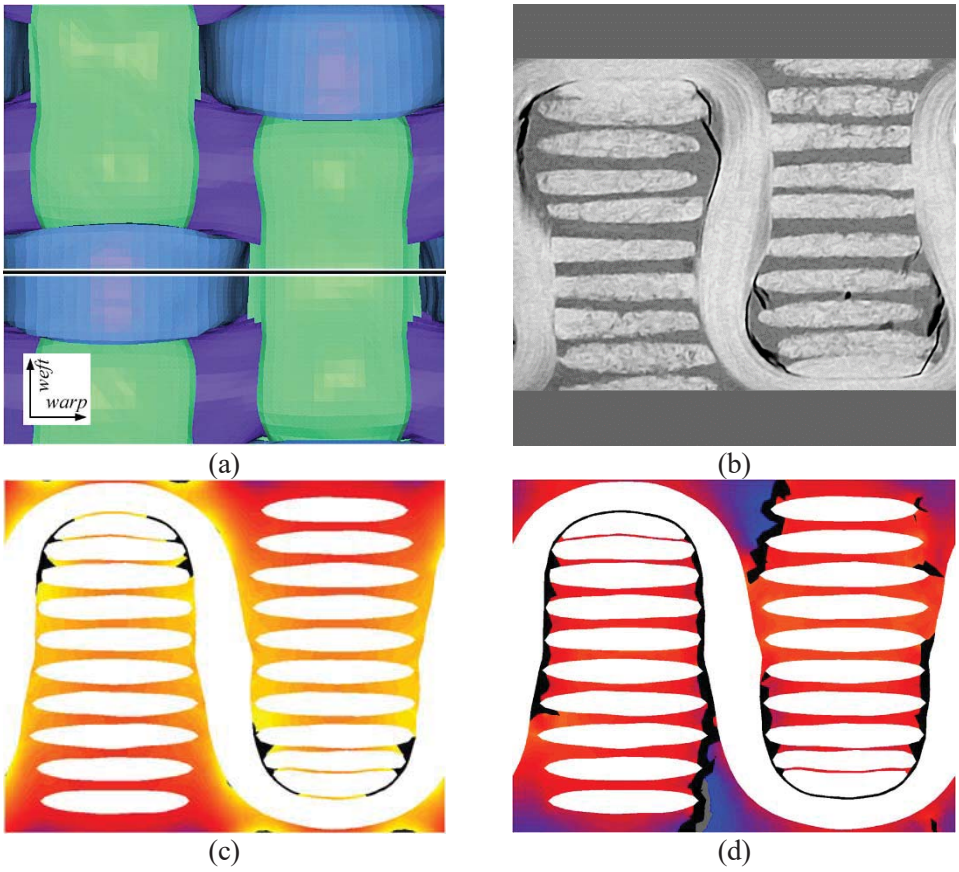

Figure 4. Propagation of damage in the 3D woven composite predicted using the parabolic stress criterion (coefficients based on [11]): (a) slice location within the UC; (b) microtomography image; (c) concentrations of the equivalent parabolic stress in an uncracked material (areas of stress above critical are shown in black); (d) cracked regions (shown in black) predicted using sequential element deactivation

CONCLUSIONS

Numerical modeling of the matrix microcracking in 3D woven composites during cooling after curing is performed using Finite Element Analysis. It was hypothesized in previous publications that the phenomenon arises as a result of high residual stresses that develop due to the mismatch in the coefficients of thermal expansion between the epoxy matrix and carbon fibers. This study was performed on the 3D woven composite with a high level of through-thickness reinforcement – the so-called one-to-one orthogonal architecture – which has been observed to be susceptible to matrix microcracking.

Four commonly used failure criteria for epoxies – von Mises, parabolic, Bauwens and dilatational energy density – were investigated for their capability to predict processing-induced damage initiation and propagation in 3D woven composites. The

predicted damage in the studied composite unit cell was compared with the X-ray computed microtomography data obtained from the actual composite specimen having the same reinforcement architecture and subjected to the same processing conditions. In addition, progressive damage was modeled via sequential element deactivation based on the parabolic stress failure criterion. The comparison of the numerical and experimental results indicated that the parabolic criterion might be the best choice for the analyzed composite system.

We conclude that the matrix microcracking phenomenon observed in 3D woven composites can be successfully modeled using the mesoscale FEA as presented in this paper, provided an appropriate failure criterion is chosen for the epoxy matrix. The approach discussed in this publication can be used to gauge the potential susceptibility of new 3D woven composite architectures before manufacturing, which could cut the R&D costs for the US composite manufacturers.

AKNOWLEDGEMENTS

This material is based upon work supported by the Materials Engineering and Processing (MEP) program of the National Science Foundation (NSF). We are grateful to Harun Bayraktar and Jon Goering (Albany Engineered Composites, Inc.) for providing the X-ray computed microtomography images of the composites with processing-induced damage and for helpful discussion of the mechanics of 3D woven composites. We acknowledge contribution of Anton Trofimov to the geometric modeling of the composite reinforcement architecture. Financial support from the New Mexico Space Grant Consortium through NASA Cooperative Agreement NNX15AK41A is also gratefully acknowledged.

REFERENCES

[1] A. Drach, B. Drach, and I. Tsukrov, "Processing of fiber architecture data for finite element modeling of 3D woven composites," *Advances in Engineering Software*, vol. 72, pp. 18–27, 2014.

[2] C. Brauner, T. Block, H. Purol, and A. Herrmann, "Microlevel manufacturing process simulation of carbon fiber/epoxy composites to analyze the effect of chemical and thermal induced residual stresses," *Journal of Composite Materials*, vol. 46, no. 17, pp. 2123–2143, 2012.

[3] R. A. Schapery, "Thermal Expansion Coefficients of Composite Materials Based on Energy Principles," *Journal of Composite Materials*, vol. 2, no. 3, pp. 380–404, Jul. 1968.

[4] Z. Hashin, "Analysis of properties of fiber composites with anisotropic constituents," *Journal of Applied Mechanics*, vol. 46, pp. 543–550, 1979.

[5] I. Tsukrov, M. Giovinazzo, K. Vyshenska, H. Bayraktar, J. Goering, and T. S. Gross, "Comparison of two approaches to model cure-induced microcracking in three-dimensional woven composites," in *Proceedings of the 2012 International Mechanical Engineering Congress & Exposition (IMECE2012)*, 2012, pp. 1–6.

[6] A. N. Gent and P. B. Lindley, "Internal Rupture of Bonded Rubber Cylinders in Tension," *Proceedings of the Royal Society A: Mathematical, Physical and Engineering Sciences*, vol. 249, no. 1257, pp. 195–205, Jan. 1959.

[7] L. E. Asp, L. Berglund, and P. Gudmundson, "Effects of a composite-like stress state on the fracture of epoxies," *Composites Science and Technology*, vol. 53, no. 1, pp. 27–37, 1995.

[8] J. W. Kim, G. a. Medvedev, and J. M. Caruthers, "Observation of yield in triaxial deformation of glassy polymers," *Polymer (United Kingdom)*, vol. 54, no. 11, pp. 2821–2833, 2013.

[9] A. Plepys, M. S. Vratsanos, and R. J. Farris, "Determination of residual stresses using incremental linear elasticity," *Composite Structures*, vol. 27, no. 1–2, pp. 51–56, 1994.
[10] T. S. Gross, H. Jafari, J. Kusch, I. Tsukrov, B. Drach, H. Bayraktar, and J. Goering, "Measuring Failure Stress of RTM6 Epoxy Resin under Purely Hydrostatic Tensile Stress using Constrained Tube Method," *Experimental Techniques*, vol. 41, no. 1, pp. 45–50, Jan. 2017.
[11] L. E. Asp, E. Marklund, J. Varna, and R. Olsson, "Multiscale modeling of non-crimp fabric composites," in *Proceedings of the 2012 International Mechanical Engineering Congress & Exposition (IMECE2012)*, 2012, pp. 1–10.
[12] T. Hobbiebrunken, M. Hojo, B. Fiedler, M. Tanaka, S. Ochiai, and K. Schulte, "Thermomechanical Analysis of Micromechanical Formation of Residual Stresses and Initial Matrix Failure in CFRP," *JSME International Journal Series A*, vol. 47, no. 3, pp. 349–356, 2004.
[13] L. E. Asp, L. A. Berglund, and R. Talreja, "A criterion for crack initiation in glassy polymers subjected to a composite-like stress state," *Composites Science and Technology*, vol. 56, no. 11, pp. 1291–1301, 1996.
[14] Y. Wang and X. Sun, "Digital-element simulation of textile processes," *Composites Science and Technology*, vol. 61, no. 2, pp. 311–319, Feb. 2001.
[15] G. Zhou, X. Sun, and Y. Wang, "Multi-chain digital element analysis in textile mechanics," *Composites Science and Technology*, vol. 64, no. 2, pp. 239–244, Feb. 2004.
[16] Y. Miao, E. Zhou, Y. Wang, and B. Cheeseman, "Mechanics of textile composites: Micro-geometry," *Composites Science and Technology*, vol. 68, no. 7–8, pp. 1671–1678, Jun. 2008.
[17] B. Drach, A. Drach, I. Tsukrov, M. Penverne, and Y. Lapusta, "Finite Element Models of 3D Woven Composites Based on Numerically Generated Micro-Geometry of Reinforcement," in *Proceedings of the American Society for Composites 2014 - 29th Technical Conference on Composite Materials*, 2014.
[18] I. Tsukrov, H. Bayraktar, M. Giovinazzo, J. Goering, T. S. Gross, M. Fruscello, and L. Martinsson, "Finite Element Modeling to Predict Cure-Induced Microcracking in Three-Dimensional Woven Composites," *International Journal of Fracture*, vol. 172, no. 2, pp. 209–216, Dec. 2011.
[19] I. Tsukrov, B. Drach, A. Drach, and T. Gross, "Utilizing Stress-Based Failure Criteria for Prediction of Curing Induced Damage in 3D Woven Composites," in *Proceedings of the Twenty First International Conference on Composite Materials – ICCM-21*, 2017.